Surface immobilization and mechanical properties of catanionic hollow faceted polyhedrons

ARTICLE · JANUARY 2006

CITATIONS
10

READS
13

7 AUTHORS, INCLUDING:

Nicolas Delorme
Université du Maine
54 PUBLICATIONS **595** CITATIONS
SEE PROFILE

Richard Weinkamer
Max Planck Institute of Colloids and Interfaces
90 PUBLICATIONS **1,704** CITATIONS
SEE PROFILE

Thomas Zemb
Institut de Chimie Séparative de Marcoule
180 PUBLICATIONS **4,853** CITATIONS
SEE PROFILE

Andreas Fery
Leibniz Institute of Polymer Research Dresden
251 PUBLICATIONS **4,843** CITATIONS
SEE PROFILE

Surface Immobilization and Mechanical Properties of Catanionic Hollow Faceted Polyhedrons

Nicolas Delorme,[†] Monique Dubois,[‡] Sébastien Garnier,[§] Andre Laschewsky,[§,||] Richard Weinkamer,[†] Thomas Zemb,[⊥] and Andreas Fery*[,†]

Max Planck Institute for Colloid and Interface Research, 14424 Potsdam, Germany, Service de Chimie Moléculaire, CEA Saclay, 91191 Gif-sur-Yvette, France, Universität Potsdam, 14415 Potsdam, Germany, Fraunhofer Institute for Applied Polymer Research FhG-IAP, D-14476 Potsdam, Germany, and Laboratoire Claude Frejacques, CNRS/CEA URA 331, DRECAM/SCM, 91191 Gif-sur-Yvette, France

Received: August 10, 2005; In Final Form: November 24, 2005

We report here for the first time on surface immobilization of hollow faceted polyhedrons formed from catanionic surfactant mixtures. We find that electrostatic interaction with the substrate dominates their adhesion behavior. Using polyelectrolyte coated surfaces with tailored charge densities, polyhedrons can thus be immobilized without complete spreading, which allows for further study of their mechanical properties using AFM force measurements. The elastic response of individual polyhedrons can be locally resolved, showing pronounced differences in stiffness between faces and vertexes of the structure, which makes these systems interesting as models for structurally similar colloidal scale objects such as viruses, where such effects are predicted but cannot be directly observed due to the smaller dimensions. Elastic constants of the wall material are estimated using shell and plate deformation models and are found to be a factor of 5 larger than those for neutral lipidic bilayers in the gel state. We discuss the molecular origins of this high stiffness.

Introduction

Above the chain melting temperature, ionic surfactants in water self-assemble into a large number of stable shapes (sphere, cylinder, bilayers, ...).[1] When cationic and anionic surfactants are mixed in water, a catanionic system is formed.[2] These catanionic systems are stabilized by the hydration force only.[3] When anionic or cationic components are added in excess, one obtains colloids of controlled surface charge, spanning from nonionic to highly charged (80 μC/cm^2) and hence highly curved mesostructures.[4]

One of the consequences of ion pairing in catanionic surfactant aggregates is an increase of 20−40 °C of the hydrophobic chain melting temperature sometimes called the "Krafft point". Stable catanionic aggregates in the crystalline state have been first proven to exist as bilayers with the shaped of nanodisks (sometimes dubbed "bicelles" of controlled size).[5] Most textbooks consider crystalline surfactant aggregates as artifacts. These rigid dispersed colloids can only be obtained in catanionic systems, since the concentration of monomers in equilibrium with "frozen micelles" lies in the range of micromoles, and not millimoles as for all other known single chain surfactant systems. The osmotic pressure, of electrostatic origin, is the dominant mechanism responsible for stability of this new kind of aggregates.[6]

Due to crystallization of hydrophobic chains, bilayer rigidity of catanionic aggregates is higher than for single surfactant components because of the ion pair forming between the surfactant heads.[7] Furthermore, in the case of the absence of additional salt (so-called "true catanionic"), strong long-range electrostatic interactions occur and lead to the formation of giant colloidal structures, showing a rich polymorphism depending on the mixing ratio.[8]

One of the most striking faceted stable shapes found is the faceted hollow polyhedron. It has been recently shown that if the edge bending energy is dominant, the free energy of formation of a polyhedron of fixed initial area is an icosahedron.[9] For this reason most of the identified objects have a local pentagonal symmetry. Since the shapes are not uniform, we design the object under investigation as a faceted polyhedron. This shape occurs with micron-sized hollow objects of well-defined thickness set by chain length.[10] This regular shape is well suited to investigating bulk material properties of these catanionic bilayers. Indeed, by mixing mystiric acid ($C_{13}H_{27}COO^-$,H^+) and cetyltrimethylammonium hydroxide ($C_{16}H_{33}N-(CH_3)_3^+$,OH^-) with an excess of the anionic component, hollow faceted polyhedrons can be formed.[6,8−11] At room temperature the chains are in the crystallized state, and freeze−fracture electron microscopic measurements[10] have shown that the faceted polyhedrons have a narrow radius distribution (from 0.7 to 2 μm) whereas combined small-angle neutron (SANS) and light scattering (SALS) experiments have demonstrated that the wall thickness of the faceted objects is 4.8 nm, corresponding to the frozen catanionic bilayer thickness. SANS has also demonstrated a surprisingly high wall rigidity since the persistence length is in the micrometer range, leading to an indirect estimation of Young's modulus (E > 100 MPa).[10]

So far, little is known on the interaction of catanionic polyhedrons with flat surfaces, and in the first part of the paper we study the interactions of the polyhedrons with different substrates and the resulting morphological changes. We find that, by using surfaces of suitable charge density, the interaction

* Corresponding author. Telephone: 49-(0)-331-567-9202. Fax: 49-(0)-331-567-9202. E-mail: andreas.fery@mpikg.mpg.de.
[†] Max Planck Institute for Colloid and Interface Research.
[‡] CEA Saclay.
[§] Universität Potsdam.
[||] Fraunhofer Institute for Applied Polymer Research.
[⊥] DRECAM/SCM.

10.1021/jp054473+ CCC: $33.50
Published on Web 01/11/2006

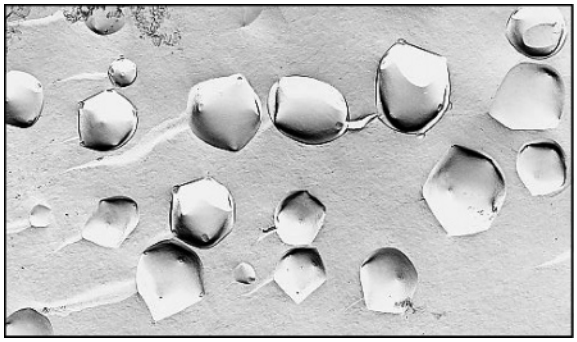

Figure 1. Freeze−fracture electron microscopic image of a solution of faceted hollow polyhedron ($r = 0.57$, $\Phi = 0.85$).

of the polyhedrons can be controlled and varied between spreading, immobilization without complete collapse, and no adhesion, which we can qualitatively explain based on ζ-potential measurements of the polyhedrons. This control of surface interactions opens novel perspectives for immobilization of the polyhedrons on surfaces[12] and could even allow array formation.[13−18] Immobilized polyhedrons can as well be studied using new characterization techniques that are not applicable in solution. We focus on the latter aspect in the second part of this paper and investigate the immobilized structures with regard to their mechanical properties using AFM (atomic force microscopy) force measurements.[19,20] As previous results showed,[10] the polyhedrons appear to be mechanically highly stable and we present data on the mechanical properties of individual immobilized hollow polyhedrons. The high lateral resolution of the force measurements allows local probing of the structure, and we find that the faceted structure leads to a reinforcement of the polyhedron. This phenomenon is also discussed as a reason for the extraordinary mechanical strength of virus structures,[21,22] but to the best of our knowledge, this is the first time that it has been directly shown for a system of colloidal dimensions.

Materials and Methods

Preparation of the Faceted Hollow Polyhedrons. The preparation of the catanionic faceted objects is well described in the literature.[8,10] The catanionic system consists of the mixing between an anionic surfactant (mystiric acid) and a cationic surfactant (cetyltrimethylammonium hydroxide, CTAOH). The composition of the system is given by the molar ratio (r) of mystiric acid to total surfactant concentration and the total surfactant concentration (Φ) in weight percent. In this study $r = 0.57$ (excess of anionic surfactant) and $\Phi = 0.85$. Freeze−fracture electron microscopy images have shown that for this composition only faceted polyhedrons were formed (Figure 1).

For the AFM measurements the initial solution was diluted to $\Phi = 0.01$ and the pH of the solution was 6.6.

Preparation of the Copolymer with Tailored Charge Density (Figure 2**).** Monomer 2-acrylamido-2-methylpropanesulfonic acid (AMPS) was a gift from Lubrizol France. Monomer *N*-[tris-(hydroxymethyl)methyl]acrylamide (TRIS) was purchased from Aldrich (purity grade 93%). Initiator 4,4′-azobis(4-cyanopentanoic carboxylate) (V-501) was obtained from WAKO. Sodium hydroxide, 1 M, was purchased from Merck. Dialysis tubes "Zellu Trans" (nominal molar mass cutoff 1000) were obtained from Roth.

In a typical procedure for the synthesis of poly(AMPS)-*co*-poly(TRIS) random copolymer (40% AMPS), an aqueous solution of AMPS (2.4013 g, 11.5870 mmol, 30 mL of water)

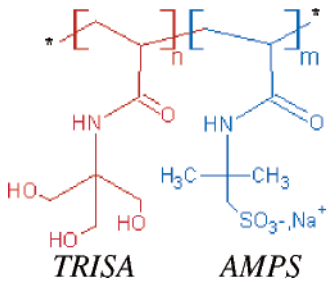

Figure 2. Structure of statistical copolymers with tailored charge density.

was first neutralized to pH 6.5 with 1 M sodium hydroxide. The aqueous neutralized AMPS solution, monomer TRIS (3.2748 g, 17.3853 mmol) and initiator 4,4′-azobis(4-cyanopentanoic carboxylate) (0.3346 g, 1.1938 mmol) were placed in a Schlenk tube. The sample was deoxygenated by N_2 bubbling for 30 min. The polymerization was performed under vigorous stirring at 60 °C and stopped after 15 h by cooling the mixture quickly to room temperature. A thick gel was obtained. The polymer was purified by dialysis in water, to remove residual monomer, and subsequently freeze-dried. The yield was 4.33 g (76.4% conversion). The analysis of the polymer was as follows. Elemental analysis: found (%) C 39.65, H 6.31, N 6.50, S 5.87. From the signal-to-noise (S/N) ratio, a molar percentage of poly(AMPS) of 39.46% was found for the random copolymer. This procedure was followed for the synthesis and characterization of homopolymers poly(AMPS) and poly(TRIS) and random copolymers poly(AMPS)-*co*-poly(TRIS) with percentages of poly(AMPS) from 10% to 90% with intervals of 10%.

Substrate Preparation. Prior to the deposition process, glass substrates were ultrasonically cleaned in methanol for 2 min followed by dipping in a Piranha solution (30% H_2O_2, 70% H_2SO_4) for 10 min. **(*CAUTION: Piranha solution is a vigorous oxidant and should be used with extreme caution.*)** After this cleaning procedure the water contact angle was near to zero, indicating that organic contamination had been eliminated.

Poly(ethylene imine) (PEI) and poly(styrenesulfonate) (PSS) were obtained from Aldrich. PEI was deposited on the cleaned glass substrate by immersion for 20 min into aqueous solution containing 10^{-2} monomol·L^{-1} (concentration in monomer units) and by rinsing with Milli-Q water. The substrate was then dried in a N_2 stream before the addition of the negatively charged polyelectrolyte.

PSS and poly(TRIS-*co*-AMPS) polylelectrolytes were deposited onto the PEI-covered glass substrate by immersion for 20 min into an aqueous solution containing 10^{-2} monomol·L^{-1} of the respective polyelectrolyte. After the deposition step the substrate was rinsed with Milli-Q water and dried in an N_2 stream.[23]

Elemental Analysis. Elemental analysis was performed with a Model EA 1110 (CHNS-O) analyzer from CE Instruments.

ζ-Potential Measurements. ζ-Potential measurements of the faceted hollow polyhedrons were performed on a Zetasizer Nanoseries (Malvern Instruments Ltd.) at 25 °C with no salt added. The apparatus transforms the electrophoretic mobility μ into a ζ-potential (mV) by using the Smoluchowski relation $\zeta = \mu\eta/\epsilon$, where η and ϵ are the viscosity and permittivity of the solution, respectively.

Atomic Force Microscopy (AFM) Measurements. All AFM images and force curves were taken with a NanoWizard AFM (JPK Instrument, Berlin) operating in contact mode in liquid by using a fluid cell (BioCell, JPK Instrument).

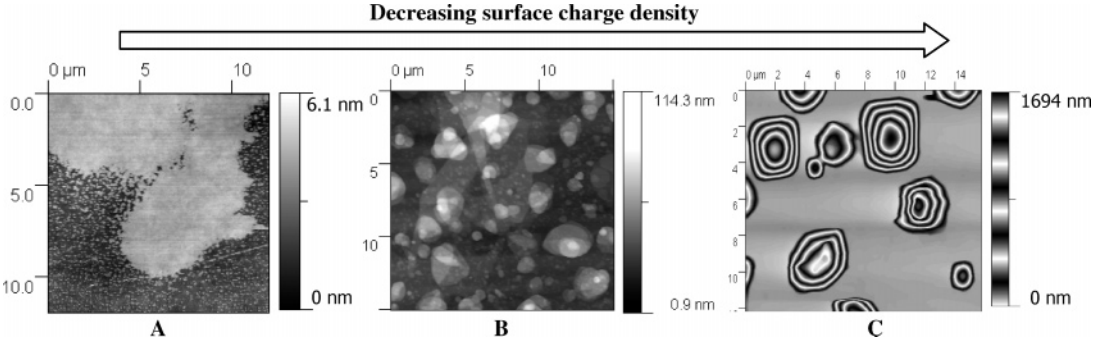

Figure 3. Height images after adsorption of faceted hollow polyhedrons on (A) cleaned glass surface, (B) poly(AMPS), and (C) poly($TRIS_{0.6}$-*co*-$AMPS_{0.4}$). In (C) a height scale of alternating black and white is used to enhance contrast.

The rectangular cantilevers (MLCT-AUNM, Veeco) used in this study had a nominal spring constant of 20 pN/nm. The spring constants were calibrated by using both thermal-oscillation[24] and Sader methods.[25] The tip radii ($R = 20-25$ nm) were measured by blind reconstruction of the tip geometry.[26] All the force−distance curves were analyzed using the software PUNIAS developed by Philippe Carl and Paul Dalhaimer.

Results and Discussion

Immobilization onto a Plane Surface. While the surface interactions of polyhedrons are little investigated, recently ζ-potential measurements showed that polyhedrons of the same mixing ratio as the ones studied here ($r = 0.57$) carry an effectively positive surface charge.[27] Although this result is surprising on first glance, since there is an excess of acidic surfactant in the mixture, it can be explained in terms of different degrees of dissociation of the surfactants.[27] We have independently carried out ζ-potential measurements and found a ζ-potential of +60 mV, confirming the past studies. This high surface charge indicates that surface interactions of the polyhedrons should be dominated by electrostatics. These results are confirmed by studies in which we incubated polyhedrons with surfaces of different surface charges and subsequently checked the substrate using imaging AFM. Indeed no adsorption was found on a positively charged surface (PEI) or on a neutral surface (glass silanized with octadecyltrichlorosilane (OTS)). In contrast, we observed a flat film (thickness ∼ 6 nm) covering a great part of the surface on freshly cleaned glass that was negatively charged (Figure 3A). Since increasing the concentration of polyhedrons in the solution resulted in a higher coverage without an increase of the film thickness, we assume that this film is the catanionic bilayer formed by spreading of the polyhedrons on the surface. Indeed it is well-known that strong interaction between lipid vesicles and the substrate can lead to the formation of an absorbed bilayer on the substrate and a similar spreading process seems to take place here.[12] The higher thickness of the film compared to the catanionic bilayer ($d \sim 4$ nm) may be due to the presence of a water layer intercalated between the bilayer and the substrate.[28]

For many applications, tailoring of the interactions such that the polyhedrons are attached, but remain uncollapsed, would be desirable. The above results clearly indicate that the control of the electrostatic interactions between substrate and polyhedron is the key parameter to achieving such immobilization. Therefore, we used statistical copolymers consisting of negatively charged 2-acrylamide-2-methylpropanesulfonic acid (AMPS) monomers and neutral trisacrylamide (TRIS) monomers to modify the surfaces used for the immobilization and to vary the charge density systematically (Figure 2). These molecules were available with different proportions of the two monomers, which is a means to vary the linear charge density of the molecules without, as shown in previous work,[23] altering their hydrophilicity at the same time. Although it is not possible to predict the effect of this variation of the linear charge density of the used molecules on the resulting surface charge density of the coated surface quantitatively, since many parameters such as molecular conformation in solution or counterion condensation phenomena are involved, the surface charge density is expected to increase monotonically with the linear charge density of the used molecule.[29,30] Thus the use of this polyelectrolyte should allow controlling the strength of the electrostatic attraction by the statistical proportion of AMPS monomers (m) in the copolymer. Indeed, as shown in Figure 3, qualitative changes in the surface morphology are observed as a consequence of reducing the linear charge density of the molecules used for surface coating.

For highly charged polyelectrolyte ($m > 0.6$), the surface morphology differs from the cleaned glass surface since structures with lateral size between 1 and 4 μm can be observed (Figure 3B). However, the measured height (∼50 nm) and the layered structure indicate that these structures were collapsed polyhedrons.

By decreasing the surface charge density ($m < 0.6$), we observed a drastic change in the surface morphology of the substrate since faceted objects of micron height can be identified on the AFM image (Figure 3C). The height of the structure is equal to its radius, indicating that the bottom parts of the faceted hollow polyhedrons are probably collapsed. Decreasing the surface charge density did not allow avoiding this partial collapse. Since the overall dimension of the faceted structures is on the order of the AFM tip itself, we took special care to rule out imaging artifacts due to tip sample convolution.[31] To confirm that the faceted structure observed on the AFM pictures is not the result of the tip convolution, we have deconvoluted the obtained AFM image by the tip geometry. For this purpose, the first step consisted in determining the tip geometry by imaging a reference sample (TGT01 from NT-MDT, Russia) formed by very sharp structures (curvature radius < 10 nm, height = 0.5 μm). In our experiment, the obtained tip geometry is a pyramid with a top angle of 50°, which is in agreement with the data given by the manufacturer. The deconvolution of the height image with the determined tip geometry was performed by using the software SPIP (from Image Metrology). By comparing the deconvoluted images with the original ones, we observed that the height and the geometry of the objects (position of the vertex, edges, ...) remained the same. Only the lateral size slightly decreased after the deconvolution operation (50−100 nm).[31] In the following, only deconvoluted images will

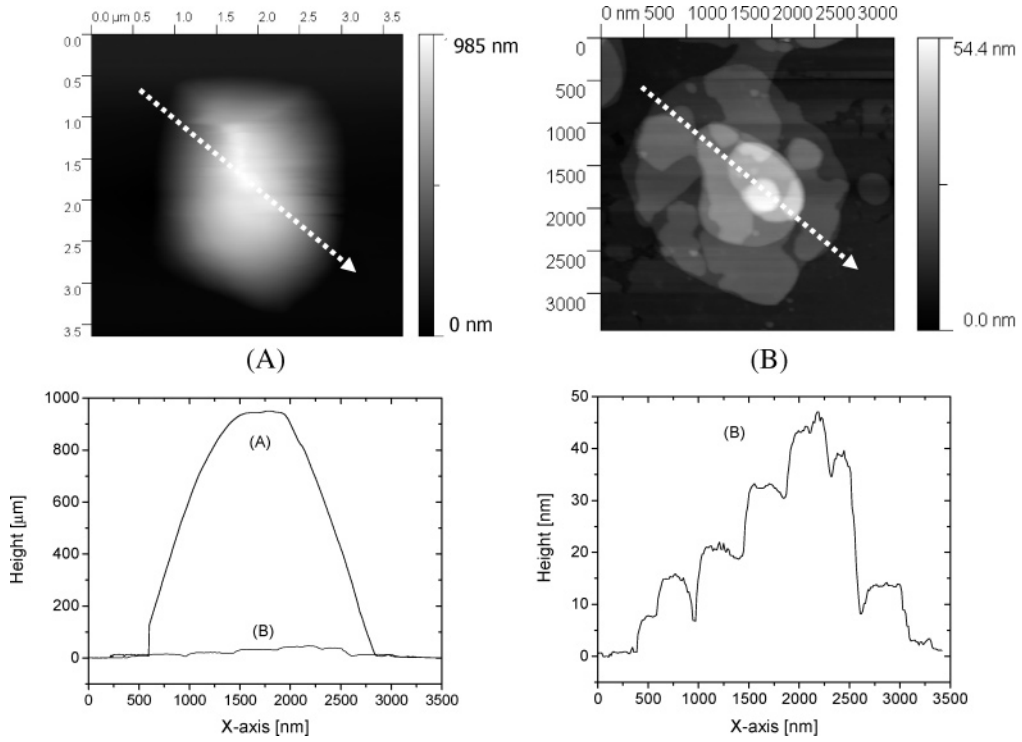

Figure 4. Height images and height profiles of the same substrate position showing a faceted hollow polyhedron (A) before and (B) after collapsing by increasing the AFM tip pressure.

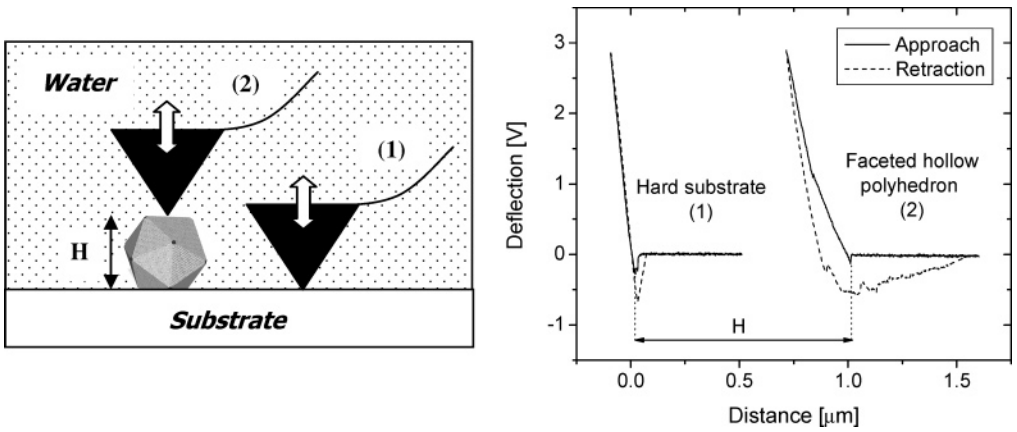

Figure 5. Principle of AFM force measurements on faceted hollow polyhedron and respective deflection-vs-distance curves taken (1) on the hard substrate to measure the sensitivity of the cantilever and (2) on the faceted object. The distance offset between the deflection-vs-distance curves (*H*) is on the same order as previously observed in the topographic imaging of the surface, which is a convenient way of avoiding/monitoring load-induced collapse.

be discussed and analysis is limited to the top, flat part of the structures which is not influenced by the tip convolution.

The hollow character of the faceted polyhedrons observed for weakly charged polyelectrolyte surface was demonstrated by increasing the pressure of the AFM cantilever on the top of a faceted object (Figure 4). This process led to the collapsing of the faceted objects into a structure near the one illustrated in Figure 3B. The cross-sectional profile clearly shows that the collapsed objects consist in a stacking of several layers having the same thickness as the observed film adsorbed onto the cleaned glass substrate ($h \sim 6$ nm) identified as the catanionic bilayer.

Preliminary studies have shown that the strength of the electrostatic interaction can also be controlled by varying other parameters such as pH or temperature and that spreading processes can be triggered by these parameters, which are similar to the ones observed here as a function of charge density. These results will be developed in a future work and published elsewhere.

Mechanical Properties. Among other perspectives, the fact that polyhedrons can be immobilized on solid surfaces without fully collapsing offers the possibility of investigating their mechanical properties by AFM force measurements with high lateral and vertical resolution. After imaging the samples in contact mode, we performed a series of force−distance investigations on selected points on the polyhedron and, for the sake of obtaining a reference from a hard surface, also on the adjacent substrate regions, as schematically depicted in Figure 5. The cantilever spring constants were calibrated as described under Materials and Methods such that absolute forces could be measured. Using the reference data on the hard surface, the cantilever deflection could be subtracted from the applied piezo displacement such that the absolute deformation of the soft structure could be measured as a function of the applied load.

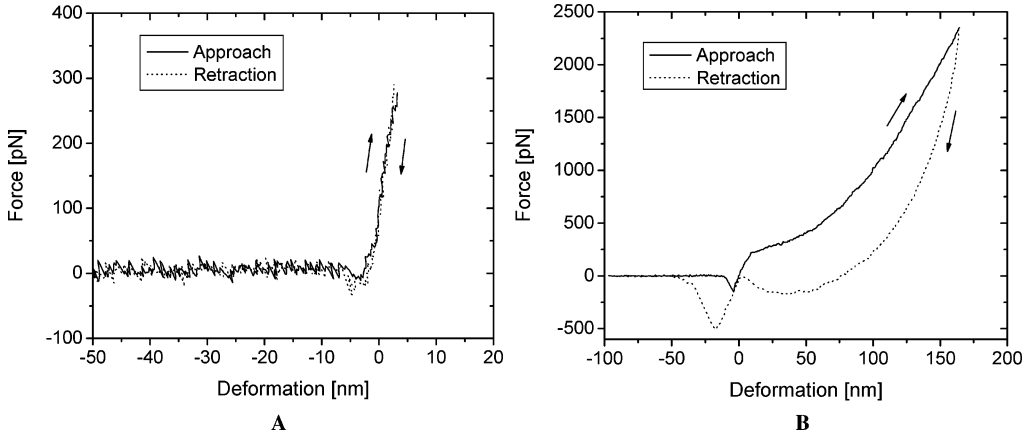

Figure 6. Force-vs-deformation curves in (A) small-deformation regime and (B) high-deformation regime of faceted hollow polyhedron adsorbed onto a poly($TRIS_{0.6}$-*co*-$AMPS_{0.4}$) surface.

In the following, only such force−deformation data (applied force versus deformation of the soft object) will be shown. In all cases, typically 50 force-vs-deformation curves for each position on a polyhedron were obtained. AFM imaging was used to check that the structure of the faceted polyhedron remains unchanged after the force-vs-distance measurements.

The qualitative features observed in the force−distance information depend strongly on the regime of deformations that are applied to the structure, as shown in Figure 6. For deformations on the order of the wall thickness, we obtained an approximately linear response of the faceted hollow polyhedrons (Figure 6A). Furthermore, the response is reversible (approaching and retracting curves superimposed), leading to the conclusion that the faceted polyhedrons have an elastic behavior in this small deformation regime.[32] For larger deformations the linear dependency of the force on the deformation is lost and a hysteresis is observed between the approaching and the retracting curves, indicating the vanishing of the elastic behavior (Figure 6B).

This behavior is typical for shell-like structures, which, other than massive particles, show a discontinuity in their deformation behavior, the buckling transition.[33] For weak deformations on the order of the wall thickness, a shell is indeed expected to show a linear force−deformation characteristic, which corresponds to a local flattening of the shell close to the contact point. As the deformation/load exceeds a critical value which is typically on the order of the wall thickness, buckling (development of indent of inverted curvature) occurs and the force−deformation characteristic becomes nonlinear.[34,35] In AFM studies of shells, the prebuckling regime has frequently been used to obtain quantitative information on elastic constants of shells.[22,32,36,37] We have recently shown that the analytic model of Reissner[38,39] compares favorably with finite element modeling of sphere deformation, and based on this model, Young's modulus of the material can be estimated by[40]

$$E_{\text{shell}} = \frac{\sqrt{3(1-\nu^2)}}{4}\frac{R}{h^2}k$$

where E_{shell} denotes Young's modulus, ν is the Poisson ratio, k is the shell stiffness (e.g., the derivative of the force−distance relation at small deformation), R is the radius of curvature of the spherical cap, and h is the wall thickness (4.8 nm). Figure 7 shows the sharp distribution of k-values, which were measured on the face of several faceted structures (∼20). Using the mean value of the measured stiffness (5 ± 0.5 pN/nm) would render an elastic modulus of 180 ± 20 MPa based on a radius of curvature of 2 μm which was obtained from the topography of the structure and a Poisson ratio of 0.33. In some cases for two-dimensional systems, zero or even negative values are found for Poisson ratios.[41,42] However, since we cannot infer the Poisson ratio from our measurement independently, we use a value characteristic of bulk materials.

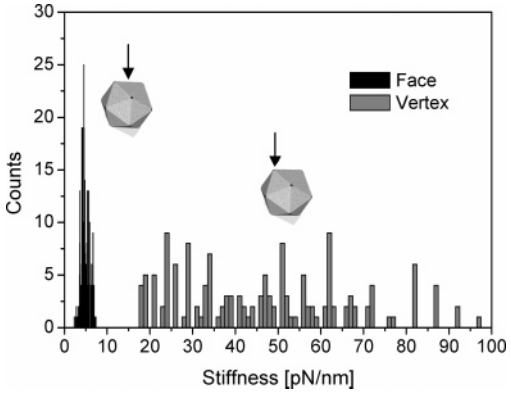

Figure 7. Stiffness measured on faces and vertexes of several faceted hollow polyhedrons adsorbed onto poly(TRIS-*co*-AMPS) surfaces with $m < 0.6$.

It has to be stressed that the value of Young's modulus depends strongly on the radius of curvature of the probed face and thus is only an order of magnitude estimate. For comparison, completely neglecting the curvature effects and using a plate model for explaining the observed stiffness would yield a higher Young's modulus of 1.3 ± 0.1 GPa, based on a Poisson ratio of 0.33 and a height of the triangular plate $a = 700$ nm obtained from the topography:[43]

$$E_{\text{plate}} = 0.069(1-\nu^2)\frac{a^2}{h^3}k$$

However, a plate model cannot account for the observed buckling instability and should also systematically overestimate the stiffness. Thus we favor the estimate of 180 ± 20 MPa based on shell theory. This result is in good agreement with previous indirect measurements that estimated Young's modulus of catanionic bilayers to be at least 100 MPa.[10]

Concluding the discussion of Young's modulus, we find a bending modulus $\kappa = Eh^3/[12(1-\nu^2)]$ [33] of the catanionic bilayer of 450 ± 50 k_BT. For uncharged floating free membranes, the bending modulus has been shown to be on the order of 275 k_BT for isolated bilayers.[44] For the catanionic bilayer the presence of surface charges increases the rigidity of the

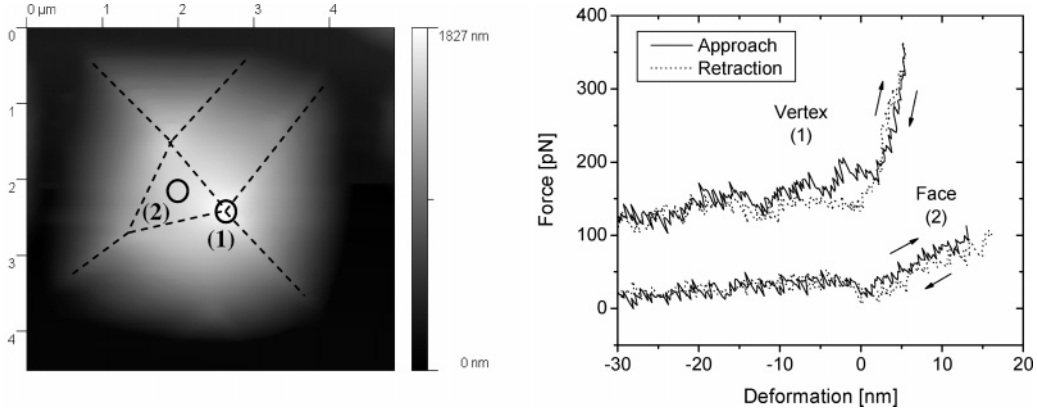

Figure 8. Height image and force-vs-deformation curves obtained on a face and on a vertex of a faceted hollow polyhedron adsorbed onto a poly($TRIS_{0.6}$-*co*-$AMPS_{0.4}$) surface. The dashed lines on the AFM pictures show the positions of the edges of the polyhedron.

bilayer due to surface networks. An increase in rigidity means an increase of the in-plane persistence length,[45] which is larger than 1 μm for catanionics while it is typically 1 order of magnitude lower for other frozen aggregates.

Neither the plate nor the shell approximation holds in the vicinity of the edges of the facets. Indeed, as shown in Figure 7, stiffness values for positions on the faces and on the edges/vertexes of the polyhedrons show pronounced differences. Figure 8 shows the correlation of stiffness and topography. The structure appears significantly stiffer when probed on vertexes ($k_{mean} \sim 50$ pN/nm) and *k*-values scatter much more as compared to the faces.

For flat faces, this result is expected from basic continuum mechanical considerations since, on the face, deformation is achieved by bending of the face in the direction of the surface normal, while in-plane compression is avoided. On the vertex, both bending and stretching occur and thus the stiffness increases. For curved faces, the situation is more complex, since bending and stretching are coupled in any case here; still the higher local curvature would also explain the observed higher stiffness due to the scaling of stiffness proportional to the inverse radius of curvature. However, analytical theories cannot quantitatively account for the observed effects in either case, and more work using finite element modeling and taking into account the full geometry of the object would be needed, which is beyond the scope of this first contribution on the subject. Still, the fact that one can resolve local differences in stiffness due to the presence of edges makes these objects potentially interesting as models for smaller colloidal faceted structures such as viruses, where such local resolution is not possible and where faceting is believed to be important for the mechanical properties as well.

Conclusion

In this paper, we have reported for the first time on surface immobilization of polyhedrons formed from catanionic surfactant mixtures. We have found that charge density of the surface used is the key parameter determining the adhesion behavior of the polyhedrons. The polyhedrons show no adhesion on positively charged or neutral surfaces, while adhesion or even spreading is found on negatively charged surfaces. This result is consistent with ζ-potential measurements, which showed a positive ζ-potential of the polyhedrons under the studied conditions. At negatively charged surfaces, we have managed to control the surface interactions via coating the surfaces using polyelectrolytes with controlled variable linear charge density. Thus, while keeping secondary interactions constant, the charge density could be varied and, depending on the linear charge density used, adhesion of hollow polyhedrons or complete spreading could be achieved. This allows, for the first time, attachment of the polyhedrons to surfaces which could have an impact on their use in applications as reaction containers or open the way for new (surface limited) techniques for their analysis.

As a first example in the latter direction, we present force measurement data on individual polyhedrons which we discuss in terms of continuum mechanical theories to estimate elastic constants of the wall material. The deformation behavior that we find for the surface immobilized hollow polyhedrons resembles that found for other shell-like systems and lets us estimate the effective elastic modulus of the wall material to be on the order of 180 ± 20 MPa ($\kappa = 450 \pm 50\ k_BT$). Due to the surface charge network, the corresponding bending modulus values are clearly larger than the one recently found for a single, lipid bilayer floating in water.

The high lateral resolution of the AFM force measurement technique allows, for the first time, direct demonstration of the impact of the faceting on the elastic response, demonstrating that the shell appears clearly stiffer (by up to 1 order of magnitude) on vertexes than on the facets. More importantly, it demonstrates that this system can serve as a model to investigate the impact of faceting on deformation, which is believed to play a crucial role in the mechanics of viruses, for which the force response cannot be laterally resolved due to their small dimensions.

Acknowledgment. We thank Helmuth Möhwald, Peter Fratzl, and David Carrière for valuable discussions and Heidi Zastrow for the ζ-potential measurements. This work was made possible by financial support from the Max-Planck Society and the Fraunhofer Society, DFG, CNRS, CEA, and the French−German Network "Complex fluids from 3D to 2D".

References and Notes

(1) Mittal, K. L.; Lindman, B. *Surfactants in solution*; Plenum Press: New York, 1984.

(2) Jokela, P.; Jonsson, B. *J. Phys. Chem.* **1988**, *92*, 1923−1927.

(3) Leikin, S.; Parsegian, V. A.; Rau, D. C.; Rand, R. P. *Annu. Rev. Phys. Chem.* **1993**, *44*, 369−395.

(4) Hyde, S.; Andersson, S.; Larsson, K.; Blum, Z.; Landh, T.; Lidin, S.; Ninham, B. *Language of shape*; Elsevier Science: Amsterdam, 1997.

(5) Zemb, T.; Dubois, M.; Demé, B.; Gulik-Krzywicki, T. *Science* **1999**, *283*, 816−819.

(6) Meister, A.; Dubois, M.; Belloni, L.; Zemb, T. *Langmuir* **2003**, *19* (18), 7259−7263.

(7) Fogden, A.; Ninham, B. W. *Adv. Colloid Interface Sci.* **1999**, *83* (1−3), 85−110.

(8) Zemb, T.; Dubois, M. *Aust. J. Chem.* **2003**, *56* (10), 971−979.

(9) Dubois, M.; Lizunov, V.; Meister, A.; Gulik-Krzywicki, T.; Verbavatz, J.-M.; Perez, E.; Zimmerberg, J.; Zemb, T. *Proc. Natl. Acad. Sci. U.S.A.* **2004**, *101*, 15082−15087.
(10) Dubois, M.; Demé, B.; Gulik-Krzywicki, T.; Dedieu, J.-C.; Vautrin, C.; Désert, S.; Perez, E.; Zemb, T. *Nature* **2001**, *411*, 672−675.
(11) Glinel, K.; Dubois, M.; Verbavatz, J. M.; Sukhorukov, G. B.; Zemb, T. *Langmuir* **2004**, *20* (20), 8546−8551.
(12) Keller, C. A.; Glasmastar, K.; Zhdanov, V. P.; Kasemo, B. *Phys. Rev. Lett.* **2000**, *84*, 5443−5446.
(13) Masson, L.; Mazza, A.; Brousseau, R. *Anal. Biochem.* **1994**, *218* (2), 405−412.
(14) Pham, D. K.; Ivanova, E. P.; Wright, J. P.; Grodzinsky, P. A.; Lenigk, R.; Nicolau, D. V. In *Surface characterization of oligonucleotides immobilized on polymer surfaces*; Nicolau, D. V., Ed.; SPIE: Bellingham, WA, 2002.
(15) Yoshina-Ishii, C.; Boxer, S. G. *J. Am. Chem. Soc.* **2003**, *125*, 3696−3697.
(16) Schonherr, H.; Rozkiewicz, D. I.; Vansco, G. J. *Langmuir* **2004**, *20*, 7308−7312.
(17) Elsner, N.; Dubreuil, F.; Fery, A. *Phys. Rev. E* **2004**, *69* (3), 031802.
(18) Nolte, M.; Fery, A. *Langmuir* **2004**, *20* (8), 2995−2998.
(19) Capella, B.; Diethler, G. *Surf. Sci. Rep.* **1999**, *34*, 1−104.
(20) Klein, D. C. G.; Stroh, C. M.; Jensenius, H.; van Es, M.; Kamruzzahan, A. S. M.; Stamouli, A.; Gruber, H. J.; Oosterkamp, T. H.; Hinterdorfer, P. *Chem. Phys. Chem.* **2003**, *4*, 1367−1371.
(21) Lidmar, J.; Mirny, L.; Nelson, D. R. *Phys. Rev. E* **2003**, *68*, 51910−51920.
(22) Ivanovska, I. L.; de Pablo, P. J.; Ibarra, B.; Sgalari, G.; MacKintosh, F. C.; Carrascosa, J. L.; Schmidt, C. F.; Wuite, G. J. L. *Proc. Natl. Acad. Sci. U.S.A.* **2004**, *101*, 7600−7605.
(23) Voigt, U.; Jaeger, W.; Findenegg, G. H.; Klitzing, R. V. *J. Phys. Chem. B* **2003**, *107* (22), 5273−5280.
(24) Hutter, J. L.; Bechhoefer, J. *Rev. Sci. Instrum.* **1993**, *64* (7), 1868−1873.
(25) Sader, J. E.; Larson, I.; Mulvaney, P.; White, L. R. *Rev. Sci. Instrum.* **1995**, *66*, 3789−3798.
(26) Villarrubia, J. S. *Surf. Sci.* **1994**, *321*, 287−300.
(27) Vautrin, C.; Zemb, T.; Schneider, M.; Tanaka, M. *J. Phys. Chem. B* **2004**, *108*, 7986−7991.
(28) Gutberlet, T.; Steitz, R.; Fragneto, G.; Klosgen, B. *J. Phys.: Condens. Matter.* **2004**, *16*, 2469−2476.
(29) Schonhoff, M. *Curr. Opin. Colloid Interface Sci.* **2003**, *8* (1), 86−95.
(30) Shafir, A.; Andelman, D. *Phys. Rev. E* **2004**, *70* (6), 061804.
(31) Leung, E. C. W.; Markiewicz, P.; Goh, M. C. *J. Vac. Sci. Technol., B* **1997**, *15* (2), 181−185.
(32) Dubreuil, F.; Elsner, N.; Fery, A. *Eur. Phys. J. E* **2003**, *12* (2), 215−221.
(33) Landau, L. D.; Lifschitz, E. M. *Theory of elasticity*; Pergamon Press: New York, 1986.
(34) Pogorelov, A. V. *Bendings of surfaces and stability of shells*; American Mathematical Society: New York, 1988.
(35) Tamura, K.; Komura, S.; Kato, T. *J. Phys.: Condens. Matter* **2004**, *16* (39), L421−L428.
(36) Helfer, E.; Harlepp, S.; Bourdieu, L.; Robert, J.; MacKintosh, F. C.; Chatenay, D. *Phys. Rev. Lett.* **2001**, *87* (8), 021904.
(37) Heuvingh, J.; Zappa, M.; Fery, A. *Langmuir* **2005**, *21* (7), 3165−3171.
(38) Reissner, E. *J. Math. Phys.* **1952**, *31* (2), 109−119.
(39) Koiter, W. T. *Proc. K. Ned. Akad. Wet., Ser. B: Phys. Sci.* **1970**, *73* (3), 169.
(40) Elsner, N.; Dubreuil, F.; Weinkamer, R.; Fischer, F. D.; Wasicek, F.; Fery, A. *Prog. Colloid Polym. Sci.* **2006**, in press.
(41) Boal, D. H.; Seifert, U.; Shillcock, J. C. *Phys. Rev. E* **1993**, *48*, 4274−4283.
(42) Spector, A. A.; Brownell, W. E.; Popel, A. S. *J. Acoust. Soc. Am.* **1998**, *103*, 1007−1012.
(43) Timoshenko, S. P.; Woinowsky-Krieger, S. *Theory of planes and shells*; McGraw-Hill: New York, 1959.
(44) Daillant, J.; Bellet-Amalric, E.; Braslau, A.; Charitat, T.; Fragneto, G.; Graner, F.; Mora, S.; Rieutord, F.; Stidder, B. *Proc. Natl. Acad. Sci. U.S.A.* **2005**, *102*, 11639−11644.
(45) Lipowsky, R.; Sackmann, E. *Structure and dynamics of membranes*; Elsevier Science: Amsterdam, 1995.